

Global Estimation for the Convoy of Autonomous Vehicles using the Sliding-mode Approach

M-Mahmoud Mohamed-Ahmed, Aziz Naamane and Nacer K. M'sirdi

Aix Marseille University, University of Toulon, CNRS, LIS UMR, Marseille, France

Keywords: Autonomous Vehicles, Convoy, State Estimation, First-Order Sliding Mode Observer, Second-Order Sliding Mode Observer, Inter-distance Estimation.

Abstract: In this paper, a global estimation approach is proposed to estimate the states of motion (longitudinal, lateral and yaw angle) of a convoy of autonomous vehicles, which is composed of four cars and also the inter-distance between each two neighboring vehicles. The approach used is based on the first-order sliding mode (FOSM) and second-order sliding mode (SOSM) observer without and with linear gain (FOSML and SOSML), to estimate and compare at the same time the estimation approach used for each vehicle in convoy. To validate this approach, we use data from SCANeRTM-Studio of a convoy moving in a defined trajectory. The robustness of the observers towards estimation errors on the model parameters will be studied.

1 INTRODUCTION

The convoy traffic is intended by the world of research and industry to ensure the safety of the infrastructure and to solve the problem of air pollution and noise due to the number of vehicles circulating in the world today. The transport of merchandise in the long way between countries as in the Chauffeur project; can move in a convoy with a driver who drives the first truck, which reduces driver fatigue. Another project, also called Sarte, has been successfully realised by the European Union, with the aim of running a convoy of autonomous vehicles at high speeds, without changing the infrastructure. Another project as Path in which a convoy of eight cars was moved at high speed on a highway. To achieve these missions; sensors are on each vehicle to get local or global information to ensure safety and complete the mission (De La Fortelle et al., 2014), (Chang et al., 1991).

In several research subjects, the problem of the convoy is particularly fixed on the longitudinal and lateral control in which all states are supposed to be measurable in real time, as in (Ali et al., 2015), (Xiang and Bräunl, 2010) and (Qian et al., 2016) in which the dynamic model is simplified to simplify the calculation of the control in real time (Avanzini et al., 2010). In (Mohamed-Ahmed et al., 2019) we proposed a coupled longitudinal and lateral control approach in order to follow a well-defined trajectory, but we also considered that the states of each vehicle

are available in real time, which represents a disadvantage in the term of observability in practice, due to the number of sensors used to calculate the law of control and to compensate for the inverse dynamics of each vehicle, which is necessary to propose an estimation of states, in order to calculate the control or to minimize the number of sensors used for a convoy of autonomous vehicles.

Slip mode estimation approaches have been proposed in the literature for one vehicle. As an example (Jaballah et al., 2011) an estimate of tyre forces has been proposed for the longitudinal movement of a tractor, based on the SOSM approach, and another estimate of the contact force is proposed (Rabhi et al., 2010) with a well-defined convergence study. ABS angle sensors were used in (M'Sirdi et al., 2008) to identify the equivalent longitudinal stiffness of the tire and the effective wheel radius of a vehicle based on the slip mode approach.

In this work, we propose a global estimation of states (position and speed) of a convoy of autonomous vehicles based on different methods of approach estimation by sliding mode. First, we will define the dynamic model used for this approach in order to represent the non-linear behavior of i -th vehicle. This model represents the longitudinal, lateral and yaw angle behaviours. In a second step, we will define the estimation method used for each vehicle. Leader is based on a first-order sliding mode observer (FOSM), the $(i - 1)$ -th vehicle uses a first-order sliding mode

observer with linear gain (FOSML). For the i -th and $(i + 1)$ -th vehicle we use a second order sliding mode (SOSM) and SOSM with linear gain (SOSML). These different methods will allow us to evaluate the most robust and efficient observer to be used in the following to control the convoy. The robustness will be studied for the presence of errors on the model parameters. To validate these approaches we use two software; SCANerTM-Studio and Matlab Simulink.

This paper is organized as follows. Section II represents the dynamic model of the longitudinal and lateral movement and yaw angle for each vehicle in the convoy. The global estimation (FOSM, FOSML, SOSM and SOSML) of the convoy is represented in section III, with the convergence study for each observer. The validation and results are presented in Section IV with the analysis of the robustness to the model parameters. The general conclusion is represented in Section V.

2 MODELING

2.1 Dynamic Model

The dynamic model is considered in this paper to estimate the movement of the fleet in the case of high speed and high curvature of the road (Rabhi, 2005). The longitudinal and lateral models are coupled and the vehicle is represented as rigid and rear-wheel driven, that is, both rear wheels are powered and the steering angles for the two wheels in front are assumed to be equal (Chebly, 2017). Let G be the center of gravity of the i -th vehicle and (G, x, y) is the vehicle's reference frame.

L_f is distance from the front wheel to G .

L_r : is the distance from the rear wheel center to G .

m, I_z : the mass and Inertia Moment of the vehicles.

m_w, I_w : the mass and the rotational inertia of the wheel.

\dot{x}, v_x : longitudinal vehicle velocity along x axis.

\dot{y}, v_y : lateral velocity (axis y).

θ : yaw angle and $\dot{\theta}$: yaw rate.

$a_x = \ddot{x} - \dot{y}\dot{\theta}$: longitudinal acceleration.

$a_y = \ddot{y} + \dot{x}\dot{\theta}$: lateral acceleration.

$C_{\alpha f}, C_{\alpha r}$: are respectively the cornering stiffness of the front and the rear wheels.

τ : driving/braking wheels torque.

δ : steering wheel angle.

$F_{aero} = \frac{1}{2}\rho c_s \dot{x}^2$: aerodynamic force, where ρ, s and c are the air density, the vehicle frontal surface and the aerodynamic constant.

R_f : radius of the tire and E : Vehicle's track.

L_3, I_3 : the interconnection between the different bodies composing the vehicle.

The dynamic model of the i -th vehicle is represented as follows (Chebly, 2017):

$$\begin{cases} m_e \ddot{x}_i - m \dot{y}_i \dot{\theta}_i + L_3 \dot{\theta}_i^2 + \delta_i (2C_{\alpha f} \delta_i - 2C_{\alpha f} \frac{\dot{x}_i(\dot{y}_i + L_f \dot{\theta}_i)}{\dot{x}_i^2 - (\dot{\theta}_i E/2)^2}) + F_{aero_i} = \frac{\tau_i}{R_f} \\ m \ddot{y}_i - L_3 \ddot{\theta}_i + m \dot{x}_i \dot{\theta}_i + 2C_{\alpha f} \frac{\dot{x}_i(\dot{y}_i + L_f \dot{\theta}_i)}{\dot{x}_i^2 - (\dot{\theta}_i E/2)^2} + 2C_{\alpha r} \frac{\dot{x}_i(\dot{y}_i - L_r \dot{\theta}_i)}{\dot{x}_i^2 - (\dot{\theta}_i E/2)^2} \\ = (2C_{\alpha f} - 2 \frac{I_w}{R_f^2} \dot{x}_i) \delta_i \\ I_3 \ddot{\theta}_i - L_3 \ddot{y}_i + 2L_f C_{\alpha f} \frac{\dot{x}_i(\dot{y}_i + L_f \dot{\theta}_i)}{\dot{x}_i^2 - (\dot{\theta}_i E/2)^2} - 2L_r C_{\alpha r} \frac{\dot{x}_i(\dot{y}_i - L_r \dot{\theta}_i)}{\dot{x}_i^2 - (\dot{\theta}_i E/2)^2} \\ - L_3 \dot{x}_i \dot{\theta}_i = L_f (2C_{\alpha f} - 2 \frac{I_w}{R_f^2} \dot{x}_i) \delta_i - (\frac{E}{2} C_{\alpha f} \frac{E \dot{\theta}_i (\dot{y}_i + L_f \dot{\theta}_i)}{\dot{x}_i^2 - (\dot{\theta}_i E/2)^2}) \delta_i \end{cases} \quad (1)$$

where: $m_e = m + 4 \frac{I_w}{R_f^2}$, $L_3 = 2m_w(L_r - L_f)$ and $I_3 = I_z + m_w E^2$.

We have two inputs for each vehicle in the convoy, which represent the inputs for the longitudinal movement (driving/braking wheels torque: $u_{xi} = \frac{\tau_i}{R_f}$) and lateral (steering wheel: $u_{yi} = (2C_{\alpha f i} - 2 \frac{I_{wi}}{R_{fi}^2} \dot{q}_{xi}) \delta_i$).

2.2 State Model

To write the i -th vehicle model as a state we will write the model in robotic form. Let q be the position vector for the three movements:

$$q_i = [q_{xi}, q_{yi}, q_{\theta i}]^T = [x_i, y_i, \theta_i]^T$$

The model presented in the equation (1) can be written as follows:

$$M_i(q_i) \cdot \ddot{q}_i + H_i(\dot{q}_i, q_i) = U_i \quad (2)$$

where the inertia Matrix $M_i(q_i)$ is:

$$M_i(q_i) = \begin{pmatrix} m_{e_i} & 0 & 0 \\ 0 & m_i & -L_{3i} \\ 0 & -L_{3i} & I_{3i} \end{pmatrix}$$

and the vector $H_i(\dot{q}_i, q_i)$ is equal to:

$$\begin{pmatrix} -m_i \dot{q}_{yi} \dot{q}_{\theta i} + L_{3i} \dot{q}_{\theta i}^2 + \delta_i (2C_{\alpha f i} \delta_i - 2C_{\alpha f i} \frac{\dot{q}_{xi}(\dot{q}_{yi} + L_{fi} \dot{q}_{\theta i})}{\dot{q}_{xi}^2 - (\dot{q}_{\theta i} E_i/2)^2}) + F_{aero_i} \\ m_i \dot{q}_{xi} \dot{q}_{\theta i} + 2C_{\alpha f i} \frac{\dot{q}_{xi}(\dot{q}_{yi} + L_{fi} \dot{q}_{\theta i})}{\dot{q}_{xi}^2 - (\dot{q}_{\theta i} E_i/2)^2} + 2C_{\alpha r i} \frac{\dot{q}_{xi}(\dot{q}_{yi} - L_{ri} \dot{q}_{\theta i})}{\dot{q}_{xi}^2 - (\dot{q}_{\theta i} E_i/2)^2} \\ 2L_{fi} C_{\alpha f i} \frac{\dot{q}_{xi}(\dot{q}_{yi} + L_{fi} \dot{q}_{\theta i})}{\dot{q}_{xi}^2 - (\dot{q}_{\theta i} E_i/2)^2} - 2L_{ri} C_{\alpha r i} \frac{\dot{q}_{xi}(\dot{q}_{yi} - L_{ri} \dot{q}_{\theta i})}{\dot{q}_{xi}^2 - (\dot{q}_{\theta i} E_i/2)^2} - L_{3i} \dot{q}_{xi} \dot{q}_{\theta i} \end{pmatrix}$$

and the input vector $U_i = (u_{xi}, u_{yi}, u_{\theta i})^T$:

$$U_i = \begin{pmatrix} \frac{\tau_i}{R_{fi}} \\ (2C_{\alpha f i} - 2 \frac{I_{wi}}{R_{fi}^2} \dot{q}_{xi}) \delta_i \\ L_{fi} u_{yi} - (\frac{E_i}{2} C_{\alpha f i} \frac{E_i \dot{q}_{\theta i} (\dot{q}_{yi} + L_{fi} \dot{q}_{\theta i})}{\dot{q}_{xi}^2 - (\dot{q}_{\theta i} E_i/2)^2}) \delta_i \end{pmatrix}$$

According to the equation (2) we can express the acceleration equation for the three motions as follows

$$\ddot{q}_i = M_i^{-1}(q_i)[-H_i(\dot{q}_i, q_i) + U_i] \quad (3)$$

In order to be able to estimate the states of three movements of each vehicle (longitudinal, lateral and yaw angle) it is interesting to write the model presented in (1) in the form of states taking as a vector of states: the position q and the speed \dot{q} .

Let z be the state of the system, we choose z :

$$z_i = (z_{1i}, z_{2i})^T = (q_i, \dot{q}_i)^T$$

with positions: $z_{1i} = q_i = [x_i, y_i, \theta_i]^T$
and velocities: $z_{2i} = \dot{q}_i = [\dot{x}_i, \dot{y}_i, \dot{\theta}_i]^T$ According to the equation (3) we have:

$$\dot{z}_{2i} = M^{-1}(z_{1i})[-H_i(z_{1i}, z_{2i}) + U_i]$$

The i -th vehicle stat model is given as follows:

$$\begin{cases} \dot{z}_{1i} = z_{2i} \\ \dot{z}_{2i} = f(z_{1i}, z_{2i}) + g(z_{1i})U_i \end{cases} \quad (4)$$

where : $f(z_{1i}, z_{2i}) = -M^{-1}(z_{1i})H_i(z_{1i}, z_{2i})$
and $g(z_{1i}) = M^{-1}(z_{1i})$

This model will be used in the following to define the observer's model and study the convergence for each vehicle in the convoy.

3 ESTIMATION

The aim of the observers, is to reconstruct the state of the position $z_1 = [x, y, \theta]^T$ using a position sensor to estimate the states of the position (z_1) and the speed (z_2) for a convoy of four vehicles. Fig. 1 shows the diagram which includes all the observers of leader, i -th, $(i - 1)$ -th and $(i + 1)$ -th vehicle.

In order to be able to estimate the states of the convoy we have the following assumptions:

Assumption . The positions z_{10}, z_{1i-1}, z_{1i} and z_{1i+1} are available in real-time.

Assumption . Model parameters $f(z_1, z_2)$ and $g(z_1)$ are measurable.

Assumption . The convoy inputs U_0, U_{i-1}, U_i and U_{i+1} are available.

3.1 Leader's Estimation: FOSM

To estimate the states of the leader a first-order sliding mode observer (FOSM) is used as shown in Fig. 1. We suppose that the position ($z_{10} = [x_0, y_0, \theta_0]^T$) and inputs such as torque and steering angle are accessible in real time.

Let $\hat{z}_{10}, \hat{z}_{20}$ be the estimated position and speed of the leader vehicle.

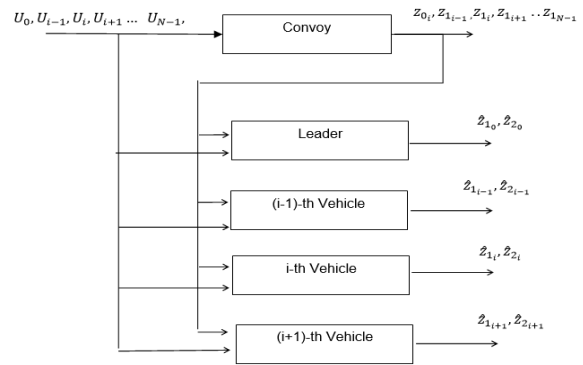


Figure 1: Principal Diagram of an observer.

The observer's model is defined as follows:

$$\begin{cases} \dot{\hat{z}}_{10} = \hat{z}_{20} - \Lambda_{10} \text{sign}(\hat{z}_{10} - z_{10}) \\ \dot{\hat{z}}_{20} = f(z_{10}, \hat{z}_{20}) + g(z_{10})U_0 - \Lambda_{20} \text{sign}(\hat{z}_{10} - z_{10}) \end{cases} \quad (5)$$

where: $f(z_{10}, \hat{z}_{20}) = -M^{-1}(z_{10})H(z_{10}, \hat{z}_{20})$.
 $\Lambda_{10} = \text{diag}(\lambda_{10}, \lambda_{10}, \lambda_{10})$ and $\Lambda_{20} = \text{diag}(\lambda_{20}, \lambda_{20}, \lambda_{20})$,
where λ_{10} and λ_{20} are positive gains.

The stability study is based on Lyapunov's approach. We define the dynamics of the error take as $\tilde{z}_{10} = \hat{z}_{10} - z_{10}$: the position error and $\tilde{z}_{20} = \hat{z}_{20} - z_{20}$: the velocity error. The error equation is defined as follows:

$$\begin{cases} \dot{\tilde{z}}_{10} = \tilde{z}_{20} - \Lambda_{10} \text{sign}(\tilde{z}_{10}) \\ \dot{\tilde{z}}_{20} = \Delta f_0 - \Lambda_{20} \text{sign}(\tilde{z}_{10}) \end{cases} \quad (6)$$

with: $\Delta f_0 = f(z_{10}, \hat{z}_{20}) - f(z_{10}, z_{20})$

Let V_0 be a function of Lyapunov candidate (Jaballah et al., 2009) :

$$V_0 = V_{10} + V_{20} \quad (7)$$

This function is divided in two parts; V_{10} to converge the state of \tilde{z}_{10} to zero and V_{20} to converge the state of \tilde{z}_{20} to zero. The first term of this function is given as follows:

$$V_{10} = \frac{1}{2} \tilde{z}_{10}^T \tilde{z}_{10}$$

By calculating the derivative of V_{10} we have :

$$\dot{V}_{10} = \tilde{z}_{10}^T (\tilde{z}_{20} - \Lambda_{10} \text{sign}(\tilde{z}_{10}))$$

We choose the gain λ_{10} :

$$\lambda_{10} > |\tilde{z}_{20}|$$

The choice of this condition ensures the convergence of \hat{z}_{10} to z_{10} in time ($t_1 > t_0$). So we'll have $\tilde{z}_{10} = 0$ for $\forall t > t_1$. From the equation 6 we can deduce the sign_e which represents the average function of the function $\text{sign} : \text{sign}_e(\tilde{z}_{10}) = \lambda_{10}^{-1} \tilde{z}_{20}$

In the equation (6) we replace the function $sign_e$ by its expression :

$$\begin{cases} \dot{\tilde{z}}_{10} = \tilde{z}_{20} - \Lambda_{10} sign_e(\tilde{z}_{10}) = 0 \\ \dot{\tilde{z}}_{20} = \Delta f_0 - \Lambda_{20} \Lambda_{10}^{-1} \tilde{z}_{20} \end{cases} \quad (8)$$

The second part of the function (V_0) is defined as:

$$V_{20} = \frac{1}{2} \tilde{z}_{20}^T \tilde{z}_{20}$$

By deriving the function V_{20} for for $t > t_1$:

$$\dot{V}_{20} = \tilde{z}_{20}^T [\Delta f_0 - \Lambda_{20} \Lambda_{10}^{-1} \tilde{z}_{20}]$$

By choosing the gain λ_{20} as follows:

$$\lambda_{20} > |\Delta f_0 \lambda_1|$$

Assuming that $|\Delta f_0| < \epsilon_0$. With these conditions we can ensure the convergence of \tilde{z}_{20} to zero in time $t_2 < t_1 < t_0$.

3.2 Estimation of $(i - 1)$ -Th Vehicle: FOSML

The preceding of i -th vehicle is estimated by FOSML (first-order sliding mode observer with a linear correction term). To define the observer model (FOSML), it is assumed that the inputs and positions for the $(i - 1)$ -th vehicle are accessible in real time. The observer model is defined (Mohamed-Ahmed et al., 2020):

$$\begin{cases} \dot{\hat{z}}_{1i-1} = \hat{z}_{2i-1} - \Lambda_{1i-1} sign(\hat{z}_{1i-1} - z_{1i-1}) \\ \quad - K_{1i-1} (\hat{z}_{1i-1} - z_{1i-1}) \\ \dot{\hat{z}}_{2i-1} = f(z_{1i-1}, \hat{z}_{2i-1}) + g(z_{1i-1}) U_{i-1} \\ \quad - \Lambda_{2i-1} sign(\hat{z}_{1i-1} - z_{1i-1}) - K_{2i-1} (\hat{z}_{1i-1} - z_{1i-1}) \end{cases}$$

where: $f(z_{1i-1}, \hat{z}_{2i-1}) = -M^{-1}(z_{1i-1})H(z_{1i-1}, \hat{z}_{2i-1})$.
 $\Lambda_{1i-1} = diag(\lambda_{1i-1}, \lambda_{1i-1}, \lambda_{1i-1})$ and $\Lambda_{2i-1} = diag(\lambda_{2i-1}, \lambda_{2i-1}, \lambda_{2i-1})$
 $K_{1i-1} = diag(k_{1i-1}, k_{1i-1}, k_{1i-1})$ and $K_{2i-1} = diag(k_{2i-1}, k_{2i-1}, k_{2i-1})$

Let $\tilde{z}_{1i-1} = \hat{z}_{1i-1} - z_{1i-1}$ position error and $\tilde{z}_{2i-1} = \hat{z}_{2i-1} - z_{2i-1}$ speed error for $(i - 1)$ -th vehicle. The dynamics of the error is given as follows:

$$\begin{cases} \dot{\tilde{z}}_{1i-1} = \tilde{z}_{2i-1} - \Lambda_{1i-1} sign(\tilde{z}_{1i-1}) - K_{1i-1} \tilde{z}_{1i-1} \\ \dot{\tilde{z}}_{2i-1} = \Delta f_{i-1} - \Lambda_{2i-1} sign(\tilde{z}_{1i-1}) - K_{2i-1} \tilde{z}_{1i-1} \end{cases} \quad (9)$$

with: $\Delta f_{i-1} = f(z_{1i-1}, \hat{z}_{2i-1}) - f(z_{1i-1}, z_{2i-1})$

To study convergence we have two possible cases:
 Case 1: $k_{1i-1} = k_{2i-1} = 0$: In this case we have an

FOSM and we can choose the Lyapunov function defined in (7) with the same convergence condition on the gains of the matrix Λ_{1i-1} et Λ_{2i-1} .

Case 2: k_{1i-1} and $k_{2i-1} \neq 0$: in this case let the following Lyapunov function:

$$V_{i-1} = V_{1i-1} + V_{2i-1} \quad (10)$$

We start to study the first part of this function (V_{1i-1}):

$$V_{1i-1} = \frac{1}{2} \tilde{z}_{1i-1}^T \tilde{z}_{1i-1}$$

This function is designed to converge the state \hat{z}_{1i-1} to the state z_{1i-1} :

$$\dot{V}_{1i-1} = \tilde{z}_{1i-1}^T (\tilde{z}_{2i-1} - \Lambda_{1i-1} sign(\tilde{z}_{1i-1}) - K_{1i-1} \tilde{z}_{1i-1})$$

First we choose the gain (λ_{1i-1}) as follows:

$$\lambda_{1i-1} > |\tilde{z}_{2i-1} - k_{1i-1} \tilde{z}_{1i-1}|$$

This condition ensures convergence of $\tilde{z}_{1i-1} = 0$ at the time ($t_1 > t_0$) and $\dot{\tilde{z}}_{1i-1} = 0$ for $\forall t > t_1$. According to the equation (9) , we can deduce the function $sign_e$:

$$sign_e(\tilde{z}_{1i-1}) = \lambda_{1i-1}^{-1} (\tilde{z}_{2i-1} - k_{1i-1} \tilde{z}_{1i-1})$$

By replacing the function $sign_e$ by its expression in the equation (9) :

$$\begin{cases} \dot{\tilde{z}}_{1i-1} = \tilde{z}_{2i-1} - \Lambda_{1i-1} sign_e(\tilde{z}_{1i-1}) - K_{1i-1} \tilde{z}_{1i-1} = 0 \\ \dot{\tilde{z}}_{2i-1} = \Delta f_{i-1} - \Lambda_{2i-1} \lambda_{1i-1}^{-1} (\tilde{z}_{2i-1} - K_{1i-1} \tilde{z}_{1i-1}) \\ \quad - K_{2i-1} \tilde{z}_{1i-1} \end{cases} \quad (11)$$

After ensuring the convergence of the state \hat{z}_{1i-1} we study the convergence of the state \hat{z}_{2i-1} based on the second term of the function (10) :

$$V_{2i-1} = \frac{1}{2} \tilde{z}_{2i-1}^T \tilde{z}_{2i-1}$$

By calculating the derivative of this function :

$$\begin{aligned} \dot{V}_{2i-1} = \tilde{z}_{2i-1}^T [\Delta f_{i-1} - \lambda_{2i-1} \lambda_{1i-1}^{-1} \tilde{z}_{2i-1} \\ + (\lambda_{2i-1} \lambda_{1i-1}^{-1} K_{1i-1} - K_{2i-1}) \tilde{z}_{1i-1}] \end{aligned}$$

This function is negative when we choose $k_{2i-1} = \lambda_{2i-1} \lambda_{1i-1}^{-1} k_{1i-1}$ and $\lambda_{2i-1} > |\Delta f_{i-1} \lambda_1|$ with $|\Delta f_{i-1}| < \epsilon_{i-1}$ and k_{1i-1} positive gain.

These conditions on the matrix gains Λ_{2i-1} and K_{2i-1} ensure the convergence of the state \hat{z}_{2i-1} to state z_{2i-1} in a time $t_2 < t_1 < t_0$.

In conclusion, the (10) is strictly negative ($\dot{V}_{i-1} < 0$) if the conditions for convergence on matrix gains are respected.

3.3 Estimation of i -Th Vehicle: SOSM

Before defining the observer model we assume that the positions ($z_{1i} = [x_i, y_i, \theta_i]^T$) and the inputs of the system (U_i) are available in real time. The nominal parameters of the model are also assumed to be measurable.

Let \hat{z}_{1i} and \hat{z}_{2i} be the estimated states. The observer model defined for the system (4) is given as follows:

$$\begin{cases} \dot{\hat{z}}_{1i} = \hat{z}_{2i} - \Lambda_{1i}|\hat{z}_{1i} - z_{1i}|^{\frac{1}{2}}\text{sign}(\hat{z}_{1i} - z_{1i}) \\ \dot{\hat{z}}_{2i} = f(z_{1i}, \hat{z}_{2i}) + g(z_{1i})U_i - \Lambda_{2i}\text{sign}(\hat{z}_{1i} - z_{1i}) \end{cases} \quad (12)$$

Λ_{1i} et Λ_{2i} are positive gains matrices defined as follows:

$$\Lambda_{1i} = \begin{bmatrix} \lambda_{1i} & 0 & 0 \\ 0 & \lambda_{1i} & 0 \\ 0 & 0 & \lambda_{1i} \end{bmatrix}$$

$$\Lambda_{2i} = \begin{bmatrix} \lambda_{2i} & 0 & 0 \\ 0 & \lambda_{2i} & 0 \\ 0 & 0 & \lambda_{2i} \end{bmatrix}$$

To study the convergence of the observer we start to write the dynamics of the error. Let $\tilde{z}_{1i} = \hat{z}_{1i} - z_{1i}$ the estimation error on the positions and $\tilde{z}_{2i} = \hat{z}_{2i} - z_{2i}$ the estimation error on the velocities. The error model is defined as follows:

$$\begin{cases} \dot{\tilde{z}}_{1i} = \tilde{z}_{2i} - |\tilde{z}_{1i}|^{\frac{1}{2}}\Lambda_{1i}\text{sign}(\tilde{z}_{1i}) \\ \dot{\tilde{z}}_{2i} = \Delta f_i - \Lambda_{2i}\text{sign}(\tilde{z}_{1i}) \end{cases} \quad (13)$$

with: $\Delta f_i = [\hat{f}(z_{1i}, \hat{z}_{2i}) - f(z_{1i}, z_{2i}) + (\hat{g}(z_{1i}) - g(z_{1i}))U_i]$

Let f_i^+ be an estimation constant such as f_i^+ :

$$\|[\hat{f}(z_{1i}, \hat{z}_{2i}) - f(z_{1i}, z_{2i}) + (\hat{g}(z_{1i}) - g(z_{1i}))U_i]\| \leq f_i^+$$

Let λ_{2i} and λ_{1i} satisfy the following conditions (Davila et al., 2005):

$$\begin{cases} \lambda_{2i} > f_i^+ \\ \lambda_{1i} > \sqrt{\frac{2}{\lambda_{2i} - f_i^+}} \frac{(\lambda_{2i} + f_i^+)(1+p)}{1-p} \end{cases} \quad (14)$$

where p is a positive constant bounded between $0 < p < 1$.

The study of the convergence of this observer is based on Lyapunov's method of choosing it as a candidate function:

$$V_i = Y_i^T R_i Y_i \quad (15)$$

This function is defined positive, continuous and non-differentiable for all $z_{1i} = 0$. (Moreno and Osorio, 2008). with:

$$Y_i = (Y_{1i}, Y_{2i})^T = (|\tilde{z}_{1i}|^{\frac{1}{2}}\text{sign}(\tilde{z}_{1i}), \tilde{z}_{2i})^T \quad (16)$$

and

$$R_i = \frac{1}{2} \begin{bmatrix} 4\Lambda_{2i} + \Lambda_{1i}^2 & -\Lambda_{1i} \\ -\Lambda_{1i} & 2 \end{bmatrix}$$

Let a_{min} : the eigenvalues of the matrix R and $\|Y\|$ the Euclidean norm, the function V is bounded between:

$$a_{min}(R)\|Y\|^2 \leq V \leq a_{max}(R)\|Y\|^2$$

Calculating the function derived from the equation (15) we find :

$$\dot{V}_i = Y_i^T R_i \dot{Y}_i + Y_i^T R_i \dot{Y}_i \quad (17)$$

The function derived from Y and according to the equation (16) is defined as follows:

$$\begin{cases} \dot{Y}_{1i} = \frac{1}{2|\tilde{z}_{1i}|^{\frac{1}{2}}} \dot{\tilde{z}}_{1i} \\ \dot{Y}_{2i} = \dot{\tilde{z}}_{2i} \end{cases} \quad (18)$$

Replacing the expression $\dot{\tilde{z}}_{1i}, \dot{\tilde{z}}_{2i}$ (13) in (18):

$$\begin{cases} \dot{Y}_{1i} = \frac{1}{2|\tilde{z}_{1i}|^{\frac{1}{2}}} (\tilde{z}_{2i} - \Lambda_{1i}|\tilde{z}_{1i}|^{\frac{1}{2}}\text{sign}(\tilde{z}_{1i})) \\ \dot{Y}_{2i} = \Delta f_i - \Lambda_{2i}\text{sign}(\tilde{z}_{1i}) \end{cases} \quad (19)$$

According with (16) we can write the equation (19) in the following form:

$$\dot{Y}_i = \frac{1}{|\tilde{z}_{1i}|^{\frac{1}{2}}} \begin{bmatrix} -\frac{\Lambda_{1i}}{2} & \frac{1}{2} \\ -\Lambda_{2i} & 0 \end{bmatrix} Y_i + \begin{bmatrix} 0 \\ 1 \end{bmatrix} \Delta f_i \quad (20)$$

As presented in the equation (14), the estimation error on the model parameters is considered to be bounded by a constant f_i^+ and the gains of λ_{1i} and λ_{2i} satisfy the conditions presented in (14).

In the following we replace (20) in the expression of the derived Lyapunov function defined in (17):

$$\dot{V}_i = -\frac{1}{|\tilde{z}_{1i}|^{\frac{1}{2}}} Y_i^T Q_i Y_i \quad (21)$$

where:

$$Q_i = \frac{\Lambda_{1i}}{2} \begin{bmatrix} 4\Lambda_{2i} + \Lambda_{1i}^2 & -\Lambda_{1i} \\ -\Lambda_{1i} & 1 \end{bmatrix}$$

Equation (21) shows that the derived Lyapunov function is strictly negative if the matrix Q is defined positive. That is, positive gains of the matrix Λ_{1i} and Λ_{2i} are chosen. This convergence condition is also granted with the conditions that are defined in equation (14) on the choice of the gains λ_{1i} and λ_{2i} according to the estimation errors on the parameters of the model.

3.4 Estimation of $(i + 1)$ -Th Vehicle: SOSML

The SOSML approach is used to reconstruct the states of $(i + 1)$ -th vehicle or the vehicle following of the (i) -th vehicle. The positions and inputs of $(i + 1)$ -th are considered to be accessible in real time. The estimation model is defined as follows:

$$\begin{cases} \dot{\hat{z}}_{1_{i+1}} = \hat{z}_{2_{i+1}} - \Lambda_{1_{i+1}} |\hat{z}_{1_{i+1}} - z_{1_{i+1}}|^{\frac{1}{2}} \text{sign}(\hat{z}_{1_{i+1}} - z_{1_{i+1}}) \\ \quad - K_{1_{i+1}} (\hat{z}_{1_{i+1}} - z_{1_{i+1}}) \\ \dot{\hat{z}}_{2_{i+1}} = f(z_{1_{i+1}}, \hat{z}_{2_{i+1}}) + g(z_{1_{i+1}}) U_{i+1} \\ \quad - \Lambda_{2_{i+1}} \text{sign}(\hat{z}_{1_{i+1}} - z_{1_{i+1}}) - K_{2_{i+1}} (\hat{z}_{1_{i+1}} - z_{1_{i+1}}) \end{cases} \quad (22)$$

where : $\Lambda_{1_{i+1}} = \text{diag}(\lambda_{1_{i+1}}, \lambda_{1_{i+1}}, \lambda_{1_{i+1}})$ and $\Lambda_{2_{i+1}} = \text{diag}(\lambda_{2_{i+1}}, \lambda_{2_{i+1}}, \lambda_{2_{i+1}})$ and $K_{1_{i+1}} = \text{diag}(k_{1_{i+1}}, k_{1_{i+1}}, k_{1_{i+1}})$ and $K_{2_{i+1}} = \text{diag}(k_{2_{i+1}}, k_{2_{i+1}}, k_{2_{i+1}})$.

Case 1: $K_{1_{i+1}} + K_{2_{i+1}} = 0$: in this case we have an second order sliding observer and the gains must satisfy the following conditions:

$$\begin{cases} \lambda_{2_{i+1}} > f_{i+1}^+ \\ \lambda_{1_{i+1}} > \sqrt{\frac{2}{\lambda_{2_{i+1}} - f_{i+1}^+}} \frac{(\lambda_{2_{i+1}} + f_{i+1}^+)(1+p)}{1-p} \end{cases} \quad (23)$$

With p is a positive constant bounded between $0 < p < 1$. f_{i+1}^+ an estimation constant such that:

$$\begin{aligned} & \| [\hat{f}(z_{1_{i+1}}, \hat{z}_{2_{i+1}}) - f(z_{1_{i+1}}, z_{2_{i+1}})] + \\ & \quad \cdot [(\hat{g}(z_{1_{i+1}}) - g(z_{1_{i+1}})) U_{i+1}] \| \leq f_{i+1}^+ \end{aligned} \quad (24)$$

To study convergence one can choose the function defined in the equation (15) which ensures the convergence in finite time with positive conditions on the gains $\lambda_{1_{i+1}}$ and $\lambda_{1_{i+1}}$.

Case 2: $K_{1_{i+1}} + K_{2_{i+1}} \neq 0$ in this case we have linear gains that improve the convergence in the finite time. The finite-time convergence of this estimation approach is proven in (Moreno and Osorio, 2008) by modifying the Lyapunov function defined in (15).

3.5 Global Estimation of the Convoy

For a convoy of four vehicles, we define the global observer, which combines several estimation approaches for different vehicles. As presented, leader uses a FOSM observer, the $(i - 1)$ -th vehicle uses a FOSML, for i -th vehicle and $(i + 1)$ -th we use an approach based on SOSM and SOSML. The global observer model is defined as follows:

$$\begin{cases} \dot{\hat{z}}_{1_0} = \hat{z}_{2_0} - \Lambda_{1_0} \text{sign}(\hat{z}_{1_0} - z_{1_0}) \\ \dot{\hat{z}}_{2_0} = f(z_{1_0}, \hat{z}_{2_0}) + g(z_{1_0}) U_0 - \Lambda_{2_0} \text{sign}(\hat{z}_{1_0} - z_{1_0}) \\ \dot{\hat{z}}_{1_{i-1}} = \hat{z}_{2_{i-1}} - \Lambda_{1_{i-1}} \text{sign}(\hat{z}_{1_{i-1}} - z_{1_{i-1}}) \\ \quad - K_{1_{i-1}} (\hat{z}_{1_{i-1}} - z_{1_{i-1}}) \\ \dot{\hat{z}}_{2_{i-1}} = f(z_{1_{i-1}}, \hat{z}_{2_{i-1}}) + g(z_{1_{i-1}}) U_{i-1} \\ \quad - \Lambda_{2_{i-1}} \text{sign}(\hat{z}_{1_{i-1}} - z_{1_{i-1}}) - K_{2_{i-1}} (\hat{z}_{1_{i-1}} - z_{1_{i-1}}) \\ \dot{\hat{z}}_{1_i} = \hat{z}_{2_i} - \Lambda_{1_i} |\hat{z}_{1_i} - z_{1_i}|^{\frac{1}{2}} \text{sign}(\hat{z}_{1_i} - z_{1_i}) \\ \dot{\hat{z}}_{2_i} = f(z_{1_i}, \hat{z}_{2_i}) + g(z_{1_i}) U_i - \Lambda_{2_i} \text{sign}(\hat{z}_{1_i} - z_{1_i}) \\ \dot{\hat{z}}_{1_{i+1}} = \hat{z}_{2_{i+1}} - \Lambda_{1_{i+1}} |\hat{z}_{1_{i+1}} - z_{1_{i+1}}|^{\frac{1}{2}} \text{sign}(\hat{z}_{1_{i+1}} - z_{1_{i+1}}) \\ \quad - K_{1_{i+1}} (\hat{z}_{1_{i+1}} - z_{1_{i+1}}) \\ \dot{\hat{z}}_{2_{i+1}} = f(z_{1_{i+1}}, \hat{z}_{2_{i+1}}) + g(z_{1_{i+1}}) U_{i+1} \\ \quad - \Lambda_{2_{i+1}} \text{sign}(\hat{z}_{1_{i+1}} - z_{1_{i+1}}) - K_{2_{i+1}} (\hat{z}_{1_{i+1}} - z_{1_{i+1}}) \end{cases} \quad (25)$$

This observer makes it possible to reconstruct the position state (longitudinal, lateral and yaw angle) to estimate the position and speed for the convoy, assuming that the model inputs and parameters are accessible in real time. The inter-distance estimates are calculated in accordance with the longitudinal position between each two neighbouring vehicles. Let $\hat{d}_{(0,i-1)} = \hat{x}_0 - \hat{x}_{i-1}$ represents the distance between leader and $(i - 1)$ -th vehicle, $\hat{d}_{(i-1,i)} = \hat{x}_{i-1} - \hat{x}_i$: between the $(i - 1)$ -th and i -th vehicle and $\hat{d}_{(i,i+1)} = \hat{x}_i - \hat{x}_{i+1}$: the inter-distance between the i -th and $(i + 1)$ -th vehicle.

4 SIMULATIONS

To validate the estimation approaches we use two software ; Scanner studio and Matlab sumilink. A convoy of four vehicles was controlled to follow a trajectory defined in Scanner Studio Fig. 2 with safe inter vehicle distances. The information is retrieved with a frequency of 20 Hz. The four observers are simulated in Matlab Simulink to validate the estimation approach and compare the results obtained by the observers with the real states of the convoy in Scaneer Studio. The chosen trajectory allows to validate the observers in the case of two movements; longitudinal and lateral (important lateral deviation as presented in Fig.3). As defined in the previous section it is assumed that longitudinal and lateral displacement and yaw angle are available in real time, as well as system inputs such as torque and steering angle for each vehicle in the convoy.

First we define the initial conditions for the states of the observer: it is supposed that $\hat{x}_0 = 0.1m$, $\hat{y}_0 = 0.5m$ and $\hat{\theta}_0 = 1rad$. The initial speeds are given as follows: $\hat{x}_0 = 1.8m/s$, $\hat{y}_0 = 0.1m/s$, $\hat{\theta}_0 = 0.1rad/s$.

The results show us in Fig. 4, the longitudinal displacement of the real and estimated convoy, the convergence time for each vehicle depends on the

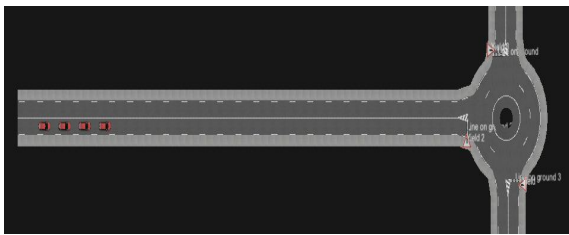


Figure 2: Trajectory Small Round.

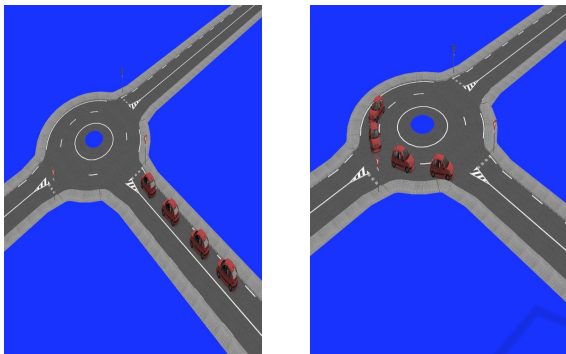


Figure 3: Movement of the convoy.

estimation approach used and the initial conditions. Fig. 5 shows us the convergence time of the error of the longitudinal displacement of each vehicle, the $(i + 1)$ -th vehicle converges faster than the other vehicles which shows the advantage of using SOSML which allows to quickly converge the estimated state to the real state by the linear gain. The $(i - 1)$ -th vehicle uses FOSML and it converges faster than the i -th vehicle (SOSM) and leader (FOSM).

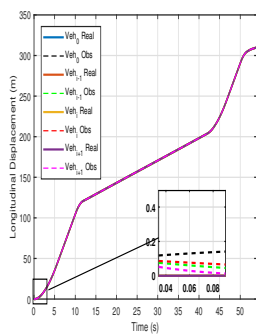


Figure 4: Longitudinal Displacement Estimation.

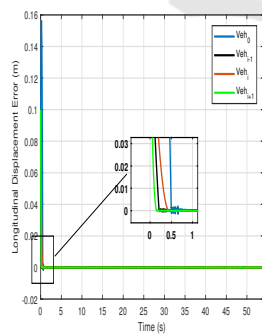


Figure 5: Longitudinal Displacement Error.

Lateral displacement is shown in Fig.6. The lateral movement is almost negligible for $t \in [0, 12\text{ s}]$ and when the convoy arrives at the crossroads Fig. 3, the convoy decreases its longitudinal speed and achieves a significant lateral deviation for $t \in [12, 42\text{ s}]$. The lateral displacement error is presented in Fig. 7, the estimated states potentially converge to the

actual states. The convergence time of the $(i + 1)$ -th vehicle SOSML is smaller than other vehicles such that $t_{i+1} < t_{i-1} < t_0$, which shows us that FOSML for $(i - 1)$ -th vehicle converges faster than SOSM without linear sheathing for the (i) -th vehicle.

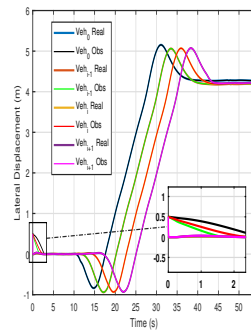


Figure 6: Lateral Displacement Estimation.

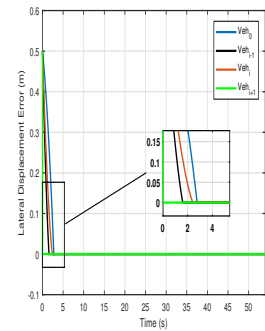


Figure 7: Lateral Displacement Error.

Fig.8 shows the yaw angles for the convoy vehicles. The initial yaw angle of the convoy observer's model is around 1 rad for each vehicle, which is influenced by the convergence time from the estimated states to the real state. In Fig.9 we see that the leader error (FOSM) converges after a duration of $t \in [0, 2\text{ s}]$ and $(i + 1)$ -th vehicle (SOSML) which is always the first one that converges to zero for a duration of 0.2 s .

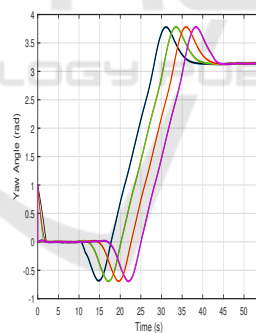


Figure 8: Yaw Angle Estimation.

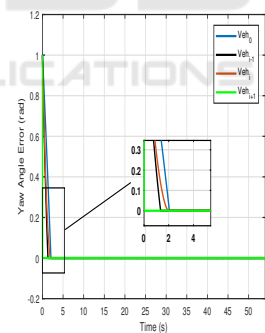


Figure 9: Yaw Angle Estimation Error.

The longitudinal speeds of the vehicles are presented in Fig.10. The speed is increased to attain 50 km/h for a longitudinal displacement such as $t \in [0, 12\text{ s}]$ and $t \in [42, 54\text{ s}]$. When the vehicles of the convoy arrive at the crossroads; the longitudinal speed is decreased to reach a speed of 10 km/h between $t \in [12, 42\text{ s}]$. The results show a rapid convergence of the estimated longitudinal speeds with the actual speeds of the convoy. It is always found that the $(i + 1)$ -th vehicle converges faster than other vehicles such that $t_{i+1} < t_{i-1} < t_0$.

The lateral speeds of the convoy are shown in

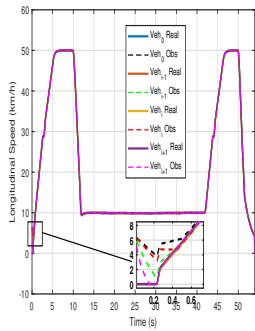


Figure 10: Longitudinal Speed.

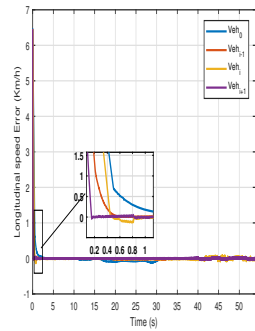


Figure 11: Longitudinal Speed Error.

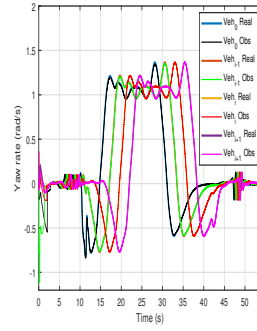


Figure 14: Yaw rate Estimation.

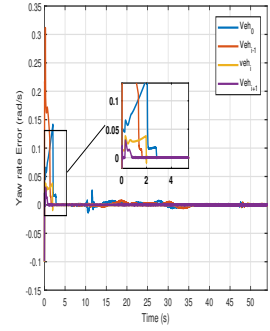


Figure 15: Yaw rate observer Error.

Fig.12. The convergence time for the leading vehicle is 3s, 2.8 s for i -th vehicle, 1.5 s for $(i - 1)$ -th vehicle and 1 s for $(i + 1)$ -th vehicle. The SOSML estimation approach for $(i + 1)$ -th vehicle is always the first one to converge to zero for the lateral speeds of the convoy according to Fig.13 . From $t \in [10 \ 35 \text{ s}]$ we find a small error for the leading and $(i - 1)$ -th vehicle, and which remains negligible for the i -th and $(i + 1)$ -th vehicle (SOSM and SOSML), which shows a robustness of the observer by second order sliding mode compared to FOSM and FOSML.

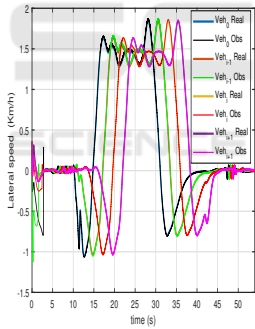


Figure 12: Lateral Speed Estimation.

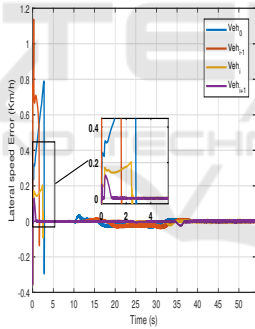


Figure 13: Lateral Speed Error.

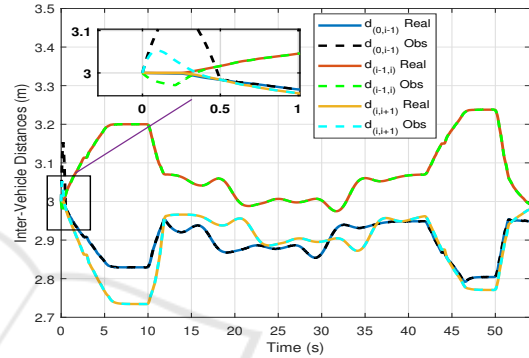


Figure 16: Inter-Vehicle distances.

the distance between the i -th vehicle and $(i + 1)$ -th vehicle ..

Fig. 16 shows us the real and estimated inters distances. The estimated distances converge quickly to the actual distances. With a speed of 50km/m the initial distance chosen between the vehicles is 3m, then a small variation of $[-0.3,0.3 \text{ m}]$ is due to the variation of the speed of the convoy.

Robustness

To test the robustness of our observers, we assume that the parameters are not well estimated, that is, we add an estimation error on the model parameters of each vehicle in the convoy. Let it be 20% of error on $f \Rightarrow \Delta f = f - \hat{f} = 20\%f$ and 20% on $g \Rightarrow \Delta g = g - \hat{g} = 20\%g$. Fig. 17 represents the error of the longitudinal displacement of the convoy, we can see that the position error is almost the same in the case of well estimated parameters (Fig. 19, Fig. 21). On the contrary, the error of the longitudinal velocity (Fig. 18) is increased in the interval $t \in [12 \ 35 \text{ s}]$. This error is also presented in the lateral velocity (Fig. 20) and yaw rate (Fig. 22)). Estimation errors for vehicles using the second order sliding mode approach are smaller than for vehicles using the first order sliding mode approach. Fig. 23 represents the inter distances

The inter-distances chosen to validate the estimation approaches are variable and the distance between the i -th vehicle and $(i - 1)$ -th vehicle is different than

of the convoy, we can see that the inter distance is almost the same in the case where the parameters are well estimated as for the three positions of the convoy. In order to improve the estimation we can modify the observer gains or decrease the initial conditions on the estimated states.

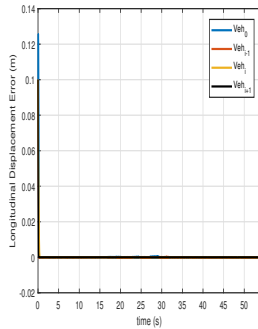


Figure 17: Longitudinal Displacement Error.

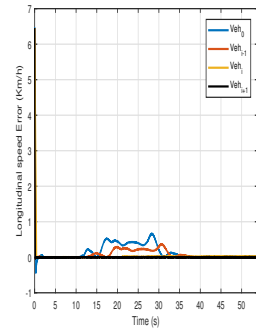


Figure 18: Longitudinal Speed Error.

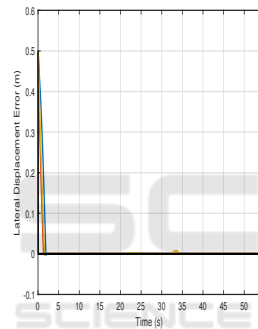


Figure 19: Lateral Displacement Error.

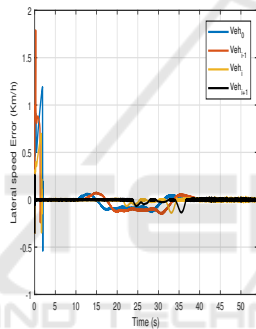


Figure 20: Lateral Speed Error.

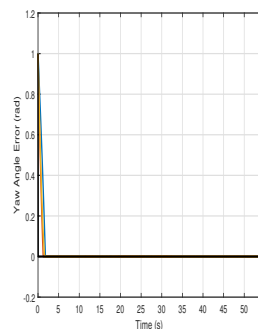


Figure 21: Yaw Angle Error.

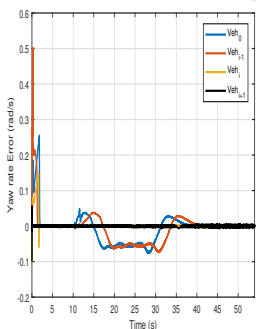


Figure 22: Yaw Rate Estimation Error.

5 CONCLUSION

In this paper, we have proposed an overall estimate for a convoy of autonomous vehicles. The four vehicles in the convoy use different estimation approaches

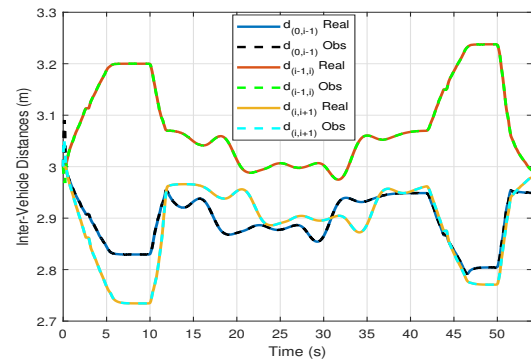


Figure 23: Inter-Vehicle distances.

to compare and select the most robust and performing observer to be used in the following to calculate the laws of longitudinal and lateral control. The developed observers estimate the positions and speeds for each movement of the convoy and the distance between the vehicles. The positions (longitudinal, lateral and yaw angle) and inputs of the convoy are assumed to be available in real-time to calculate the observers' models. Practical validation using SCANerTM-Studio data shows the rapid convergence of estimated states to real states and the robustness of this approach against estimation errors on the convoy model parameters. The vehicles using linear gain sliding mode observers (FOSML and SOSML) converge rapidly compared to vehicles without linear gain observers (FOSM and SOSM), but when the model parameters are not well estimated; the estimation errors of the vehicles using the second-order sliding mode approach (SOSM and SOSML) are smaller than the other vehicles (FOSM and FOSML). The trajectory chosen for the movement of the convoy makes it possible to test the approach developed in the case of a large radius of curvature and average longitudinal speed.

REFERENCES

Ali, A., Garcia, G., and Martinet, P. (2015). Urban platooning using a flatbed tow truck model. In *Intelligent Vehicles Symposium (IV), 2015 IEEE*, pages 374–379. IEEE.

Avanzini, P., Thuilot, B., and Martinet, P. (2010). Accurate platoon control of urban vehicles, based solely on monocular vision. In *Intelligent Robots and Systems (IROS), 2010 IEEE/RSJ International Conference on*, pages 6077–6082. IEEE.

Chang, K. S., Li, W., Devlin, P., Shaikhbahai, A., Varaiya, P., Hedrick, J. K., McMahon, D., Narendran, V., Swaroop, D., and Olds, J. (1991). Experimentation with a vehicle platoon control system. In *Vehicle Navigation*

- and *Information Systems Conference, 1991*, volume 2, pages 1117–1124.
- Chebly, A. (2017). *Trajectory planning and tracking for autonomous vehicles navigation*. PhD thesis, Université de Technologie de Compiègne.
- Davila, J., Fridman, L., and Levant, A. (2005). Second-order sliding-mode observer for mechanical systems. *IEEE transactions on automatic control*, 50(11):1785–1789.
- De La Fortelle, A., Qian, X., Diemer, S., Grégoire, J., Moutarde, F., Bonnabel, S., Marjovi, A., Martinoli, A., Llatser, I., Festag, A., et al. (2014). Network of automated vehicles: the autonet 2030 vision.
- Jaballah, B., M'sirdi, N., Naamane, A., and Messaoud, H. (2009). Estimation of longitudinal and lateral velocity of vehicle. In *2009 17th Mediterranean Conference on Control and Automation*, pages 582–587. IEEE.
- Jaballah, B., M'sirdi, N. K., Naamane, A., and Messaoud, H. (2011). Estimation of vehicle longitudinal tire force with fosmo & sosmo. *International Journal on Sciences and Techniques of Automatic control and computer engineering, IJSTA*, page à paraître.
- Mohamed-Ahmed, M., M'sirdi, N., and Naamane, A. (2020). Non-linear control based on state estimation for the convoy of autonomous vehicles. In *ICCARV 2020: 14ème International Conference on Control Automation Robotics and Vision*.
- Mohamed-Ahmed, M., Naamane, A., and M'sirdi, N. (2019). Path tracking for the convoy of autonomous vehicles based on a non-linear predictive control. In *THE 12TH International Conference on Integrated Modeling and Analysis in Applied Control and Automation*.
- Moreno, J. A. and Osorio, M. (2008). A Lyapunov approach to second-order sliding mode controllers and observers. In *2008 47th IEEE conference on decision and control*, pages 2856–2861. IEEE.
- M'Sirdi, N., Rabhi, N., Fridman, A., Davila, L., and Delanne, J. (2008). Second order sliding-mode observer for estimation of vehicle dynamic parameters.
- Qian, X., Altch, F., de La Fortelle, A., and Moutarde, F. (2016). A distributed model predictive control framework for road-following formation control of car-like vehicles. In *arXiv:1605.00026v1 [cs.RO] 29 Apr 2016*.
- Rabhi, A. (2005). *Estimation de la dynamique du véhicule en interaction avec son environnement*. PhD thesis, Versailles-St Quentin en Yvelines.
- Rabhi, A., M'Sirdi, N., Naamane, A., and Jaballah, B. (2010). Estimation of contact forces and road profile using high-order sliding modes. *International Journal of Vehicle Autonomous Systems*, 8(1):23–38.
- Xiang, J. and Bräunl, T. (2010). String formations of multiple vehicles via pursuit strategy. *IET control theory & applications*, 4(6):1027–1038.